Earth System
Dynamics

Open Access

EGU

Supplement of

Carbon cycle and climate feedbacks under CO_2 and non-CO_2 overshoot pathways

Irina Melnikova et al.

*Correspondence to:* Irina Melnikova (melnikova.irina@nies.go.jp)

15 **Table S1. Changes in the carbon cycle feedback parameters for land and ocean at the end of the ramp-up period, shown as three-member ensemble mean. The ± indicates one standard deviation among the three members. We use temperature of the fully coupled experiments to estimate γ and χ feedbacks.**

| Experiment	Terms	Years 1-50 (ramp-up)	
		Land	Ocean
[CO_2bgc]	β_{CO2} (GtC ppm^{-1})	1.51 ± 0.02	0.88 ± 0.01
[CO_2rad]	γ_{CO2} (GtC K^{-1})	-17.02 ± 1.44	-2.17 ± 0.14
[nonCO_2]	γ_{nonCO2} (GtC K^{-1})	-16.74 ± 4.12	-2.58 ± 1.19
[CO_2] - [CO_2bgc] - [CO_2rad]	χ_{CO2} (GtC ppm^{-1} K^{-1})	0.03 ± 0.02	-0.02 ± 0.0
[nonCO_2bgc] - [CO_2bgc] - [nonCO_2]	χ_{nonCO2} (GtC ppm^{-1} K^{-1})	0.03 ± 0.01	-0.01 ± 0.01
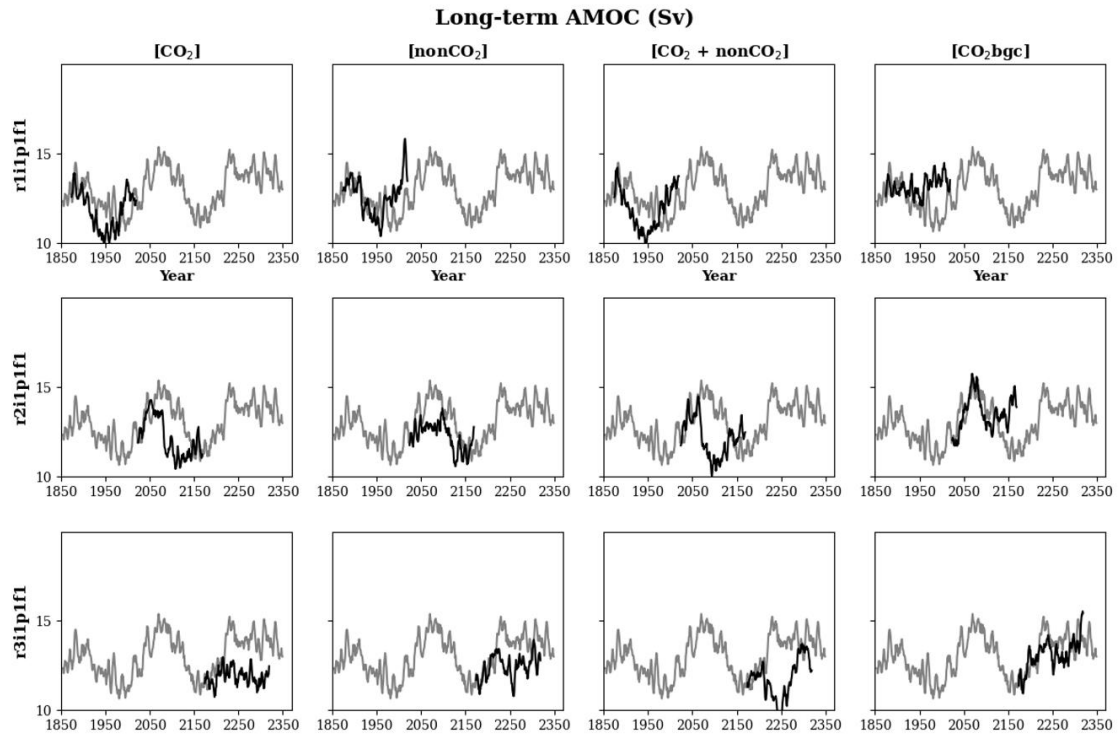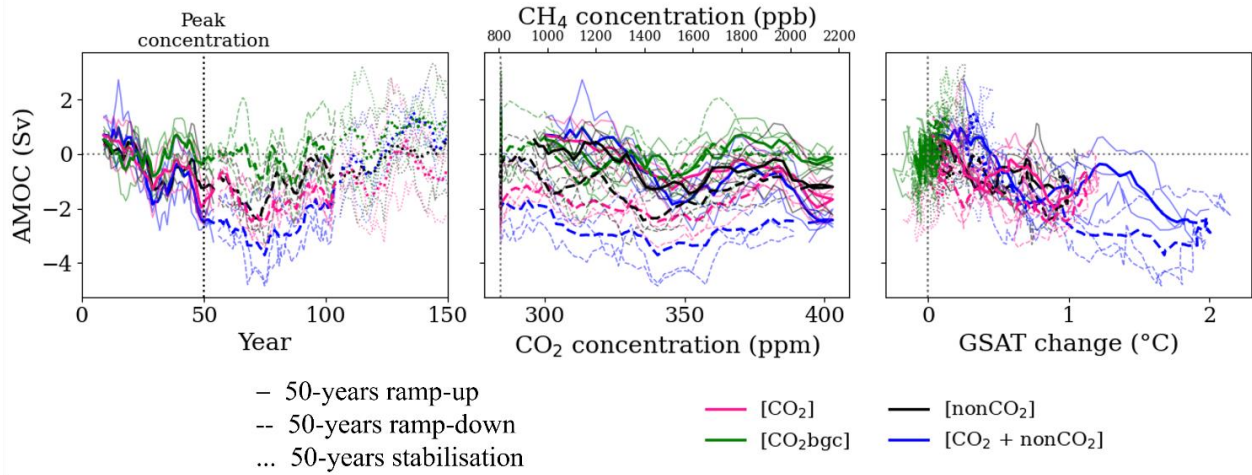
Figure S1. (a) Comparison of the Atlantic Meridional Overturning Circulation (AMOC) time evolution in the IPSL-CM6A-LR idealised experiments relative to the initial date in the pre-industrial control simulation. Time evolution of the 5-year moving average AMOC (Sv) from the piControl simulation (grey) and from the idealised experiments. (b) AMOC as a function of time (year), CO_2 concentration (ppm) / CH_4 concentration (ppb, only for [nonCO2]), and GSAT (ºC) under selected scenarios. Thick lines indicate the ensemble means and thin lines correspond to three ensemble members.

3
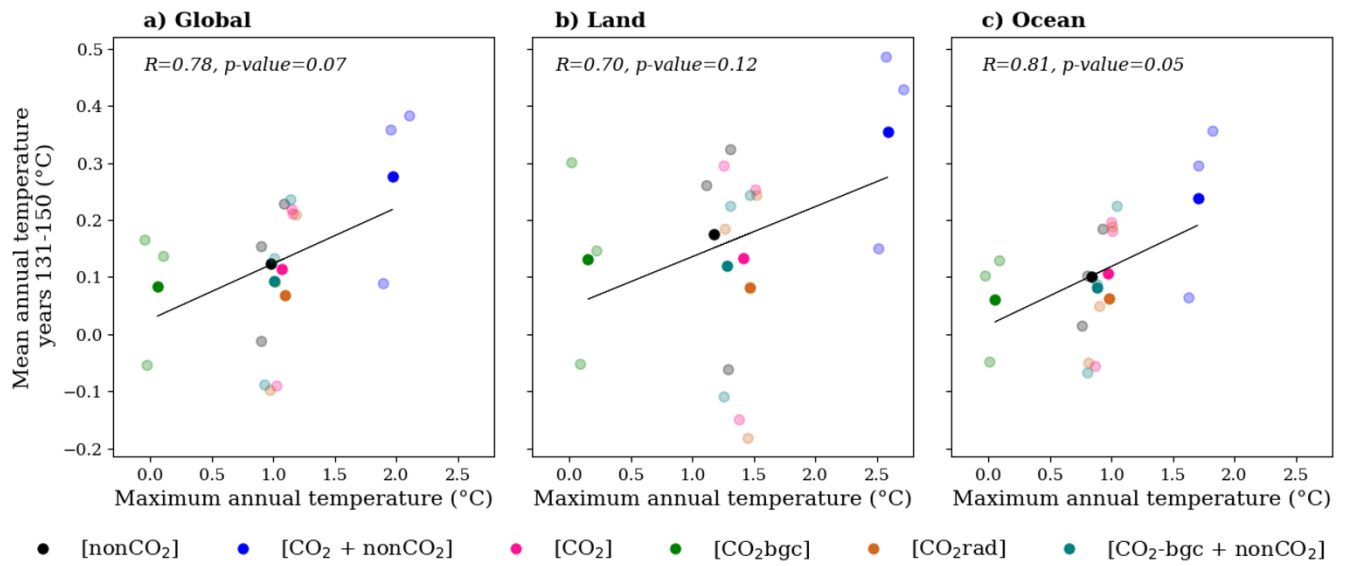
Figure S2. (a) Global, (b) land and (c) ocean mean annual surface averaged over the last 20 years of each experiment plotted against corresponding maximum annual temperature for each experiment and each ensemble member (transparent dots) and ensemble means (solid dots). The correlation coefficients are calculated for ensemble means.

30

a)

b)
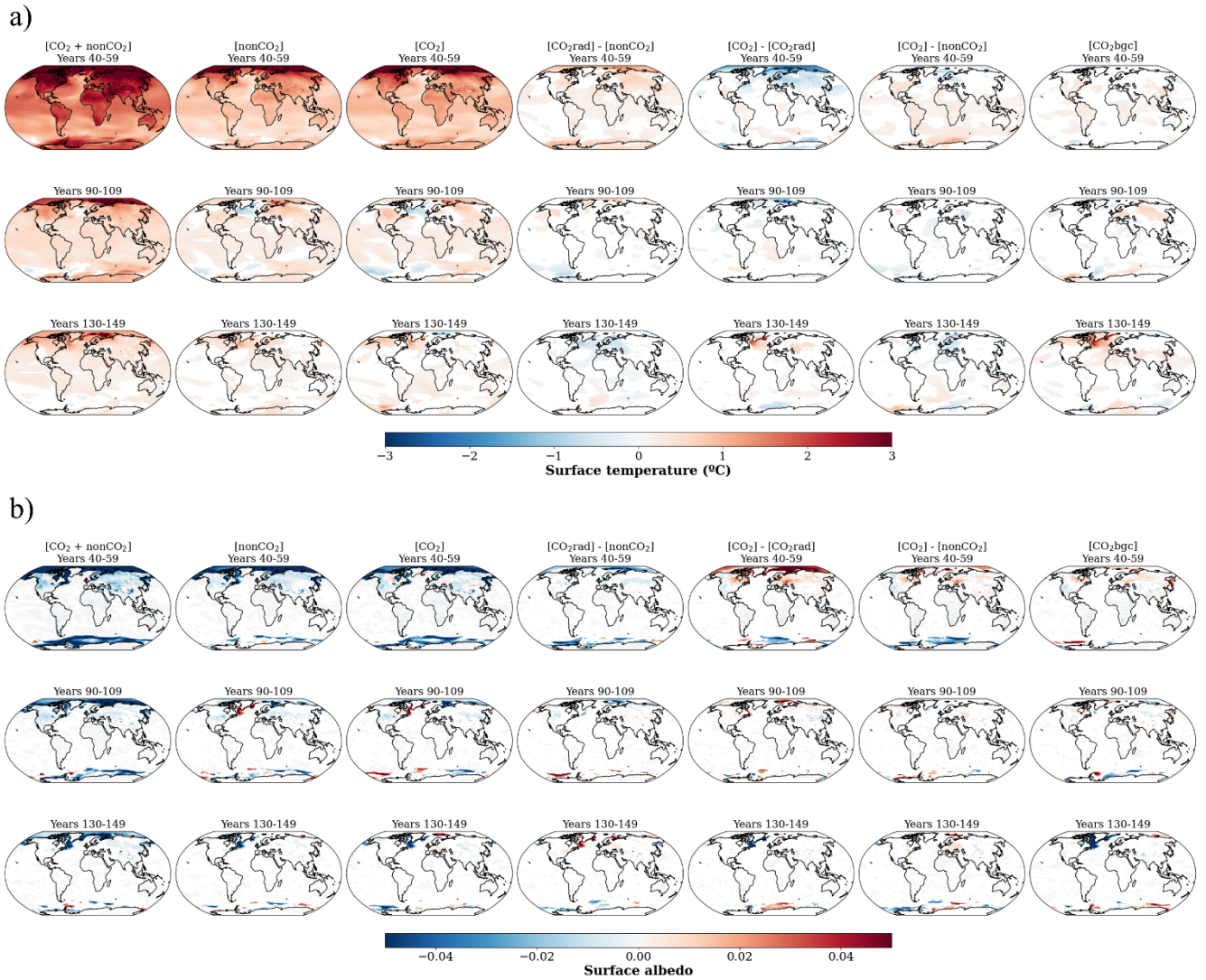
Figure S3. Spatial variation of three-member-ensemble mean changes in (a) surface temperature (ºC) and (b) surface albedo averaged over 20 years at the end of (first rows) ramp-up, (middle rows) ramp-down, and (bottom rows) stabilisation phases relative to piControl under selected scenarios. We draw only grids significantly different from piControl ($p < 0.1$ based on t test, N=60) and between [CO_2], [CO_2rad] and [$nonCO_2$] experiments using three ensemble members ($p < 0.1$ based on t test, N=60).

5
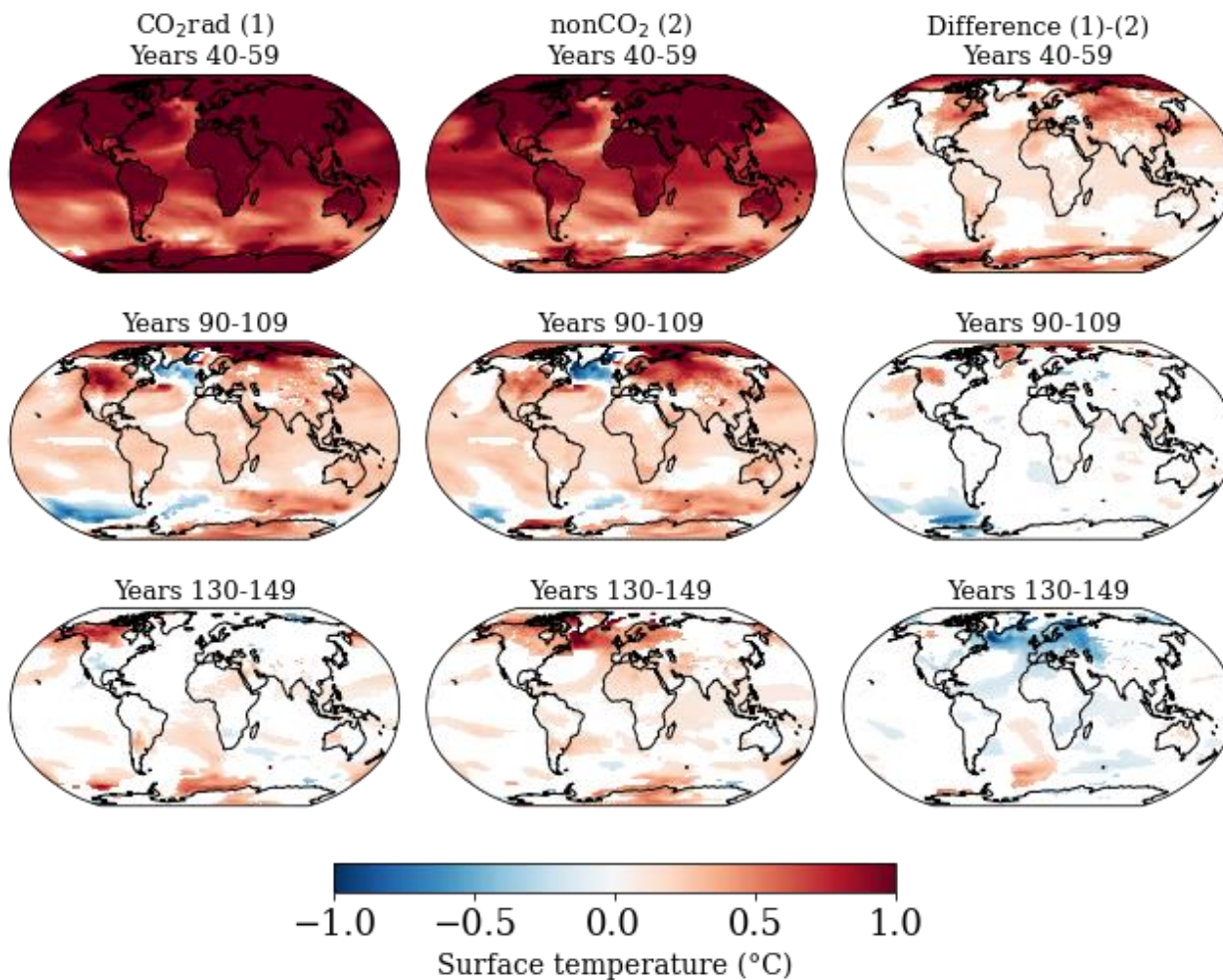
Figure S4. Spatial variation of three-member-ensemble mean changes in surface temperature (℃) averaged over 20 years at the end of (first rows) ramp-up, (middle rows) ramp-down, and (bottom rows) stabilisation phases in the [CO_2rad] and [nonCO_2] experiment. We draw only significantly different grids using three ensemble members ($p < 0.1$ based on t test, N=60).
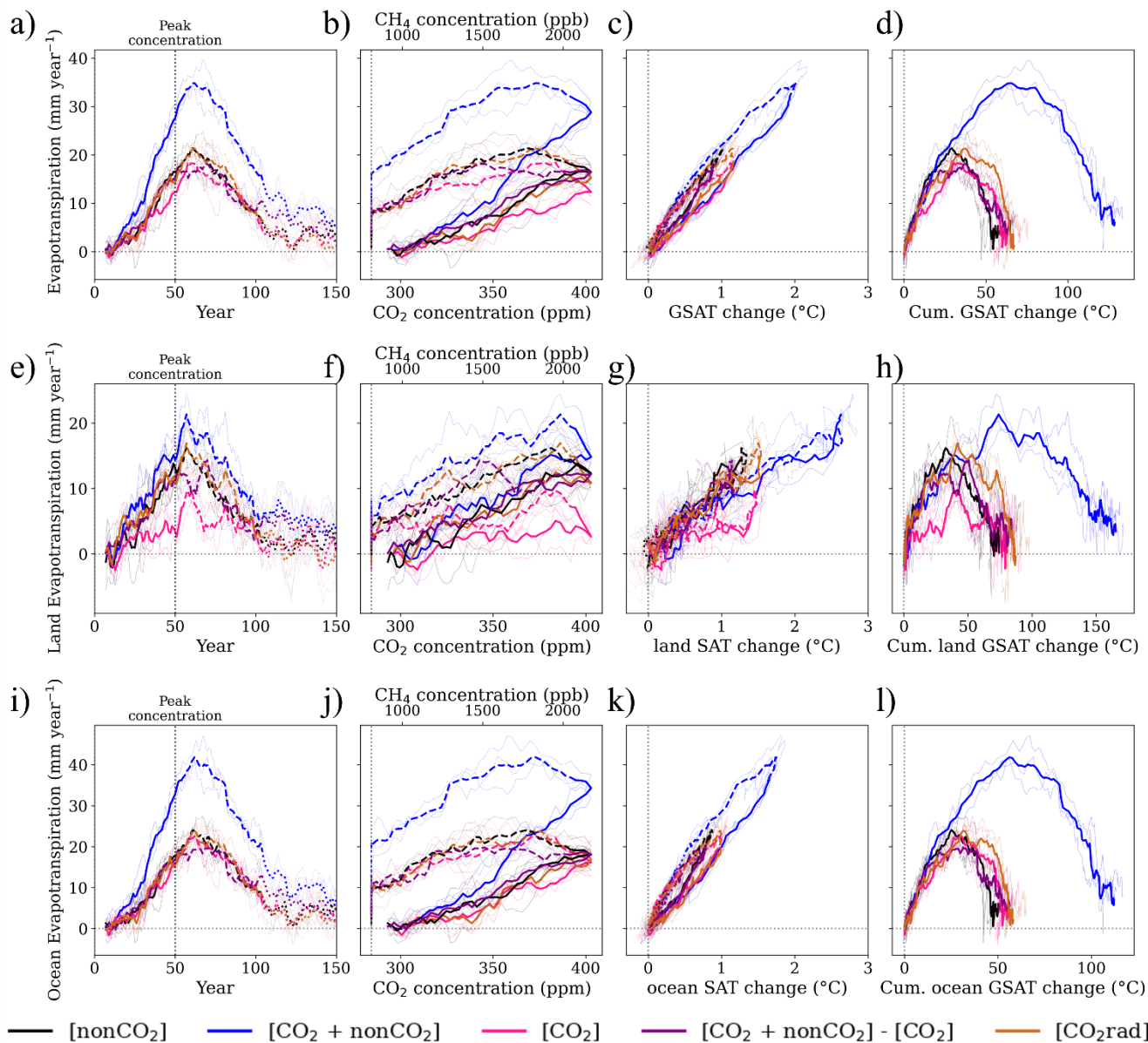
Figure S5. (a–d) Global, (e–h) land and (i–l) ocean annually-averaged changes in evapotranspiration (mm year^{-1}) as a function of (a, e, i) time (year), (b, f, j) CO_2 concentration (ppm) / CH_4 concentration (ppb, only for [nonCO$_2$]), (c, g, k) GSAT (ºC) and (d, h, l) cumulative GSAT (ºC).
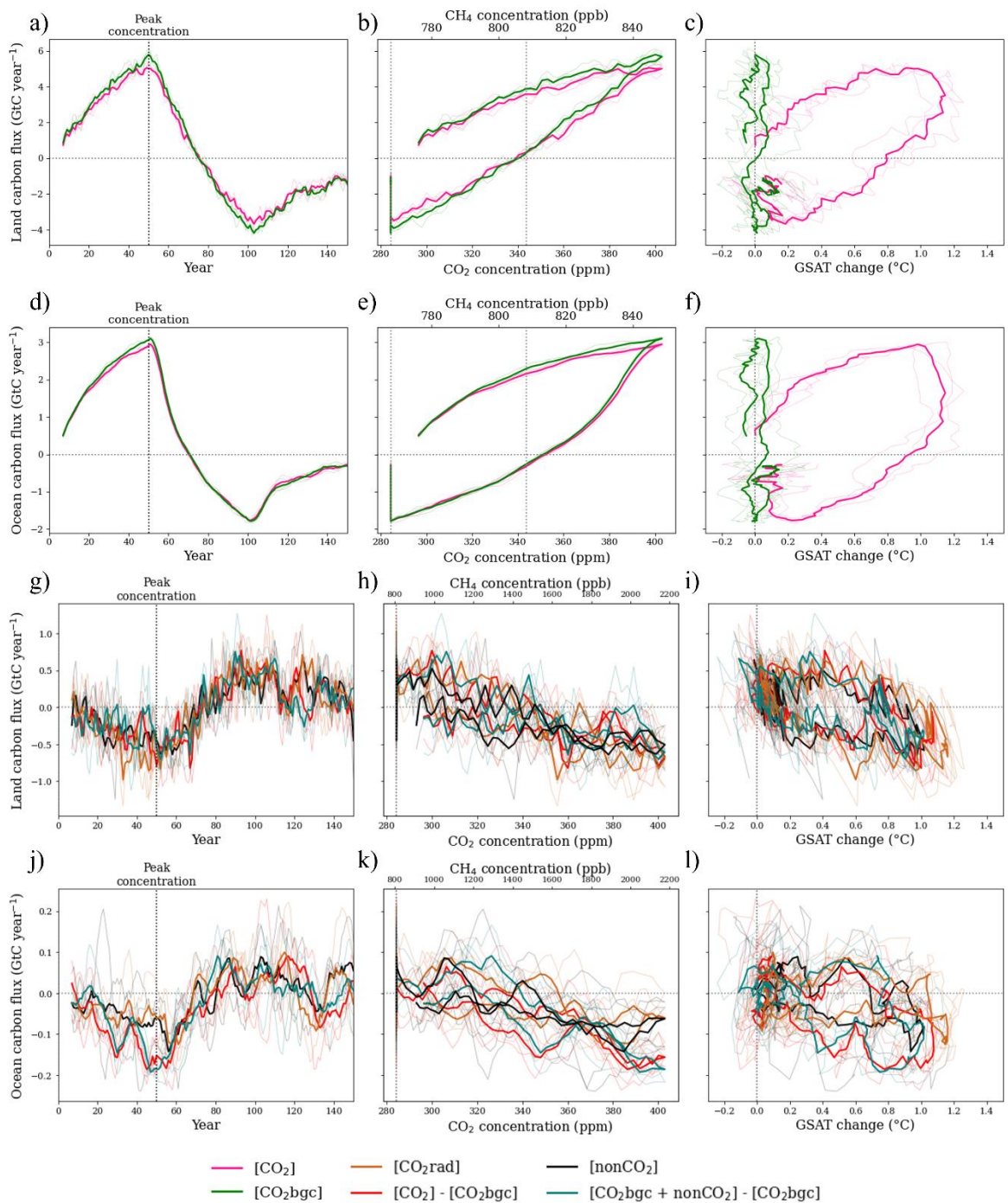
Figure S6. Global (a–c, g–i) land and (d–f, j–l) ocean carbon flux, positive sink to the land/ocean (GtC year^{-1}) as a function of (a, d, g, j) time (year), (b, e, h, k) CO$_2$ concentration (ppm) / CH$_4$ concentration (ppb, only for [nonCO$_2$]) and (c, f, i, l) GSAT (ºC) under selected scenarios.

55

8
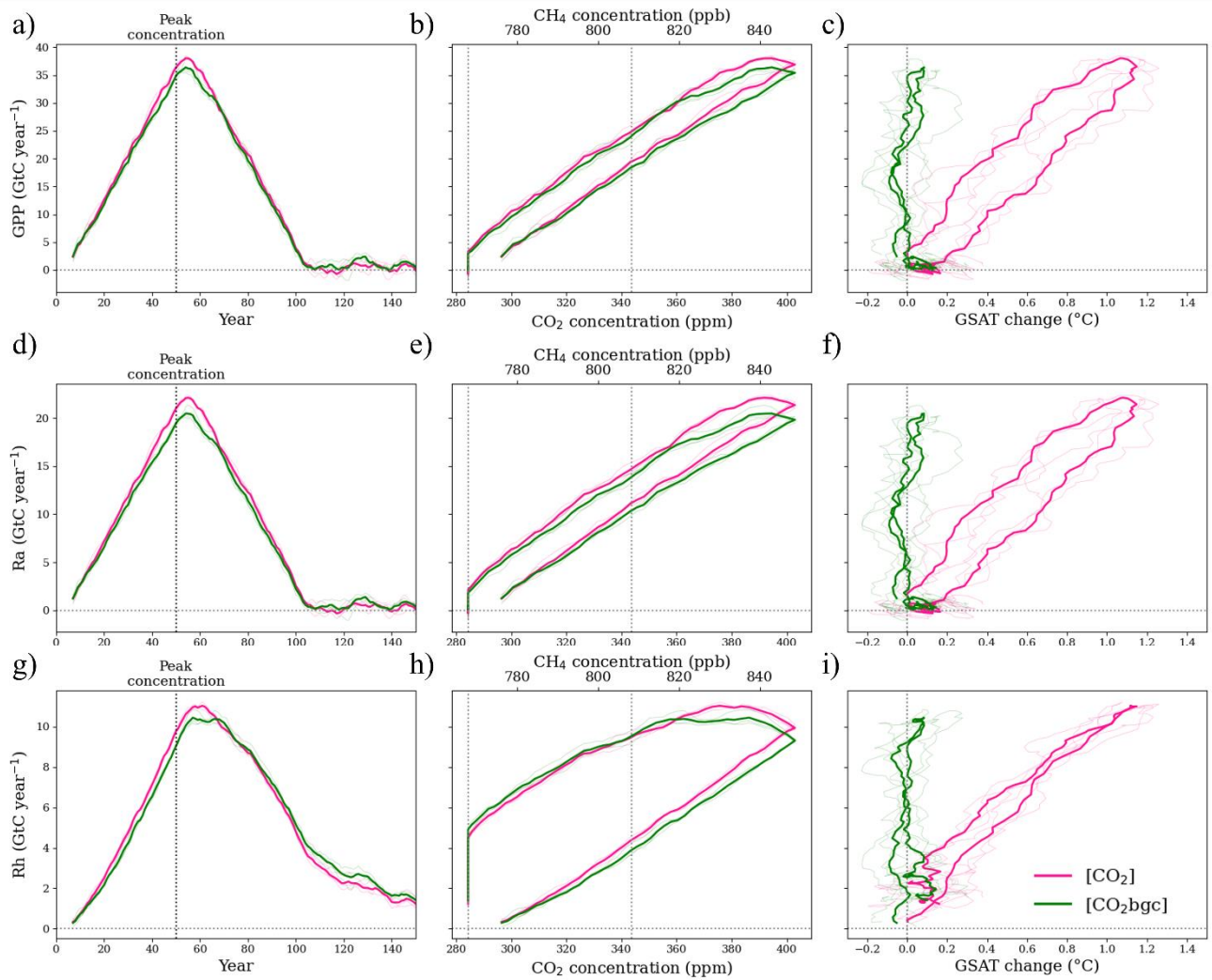
Figure S7. Global (a–c) GPP, (d–f) Ra and (g–i) Rh (GtC year⁻¹) as a function of (a, d, g) time (year), (b, e, h) CO_2 concentration (ppm) / CH_4 concentration (ppb, only for [nonCO₂]) and (c, f, i) GSAT (°C) under selected scenarios.
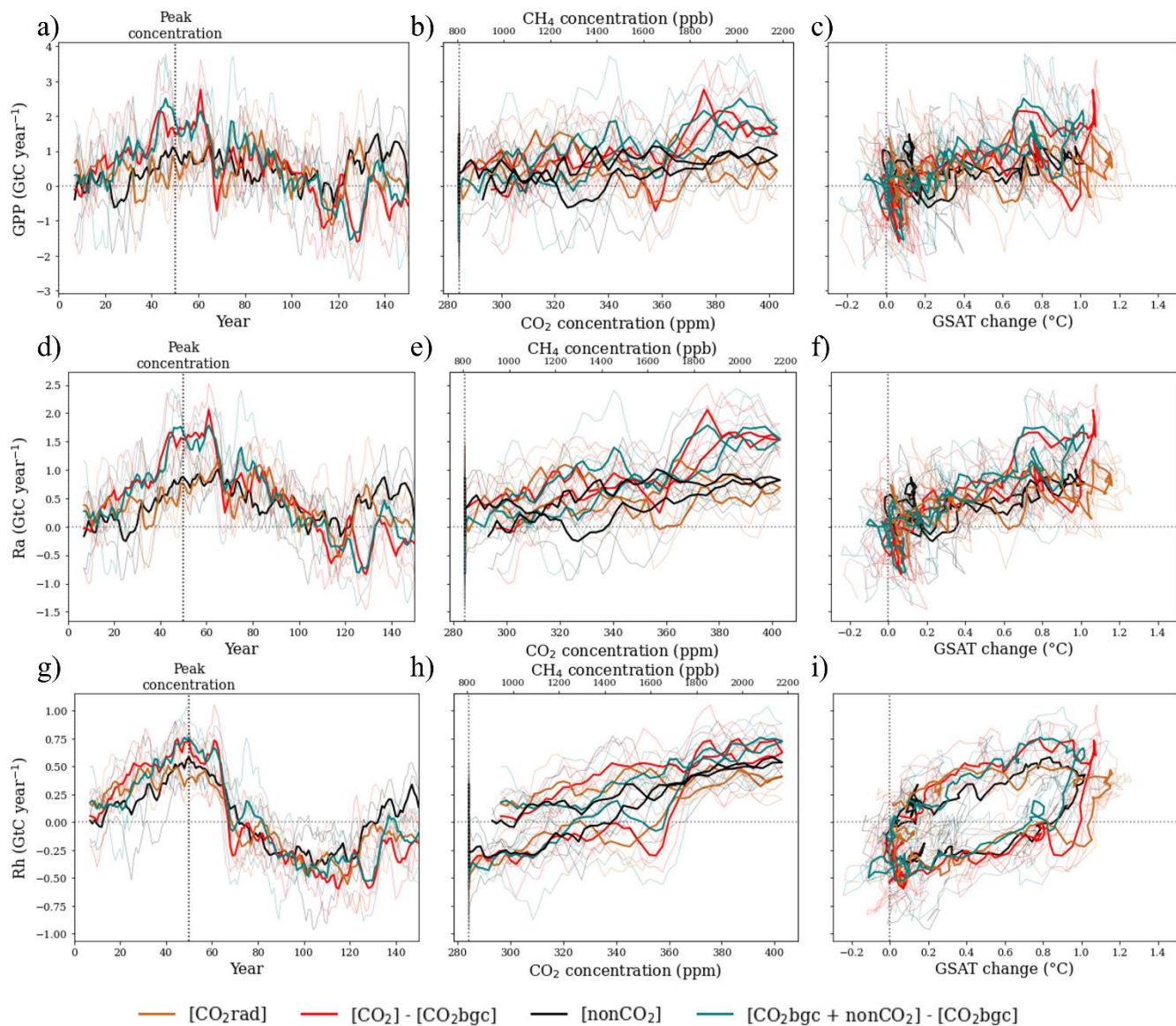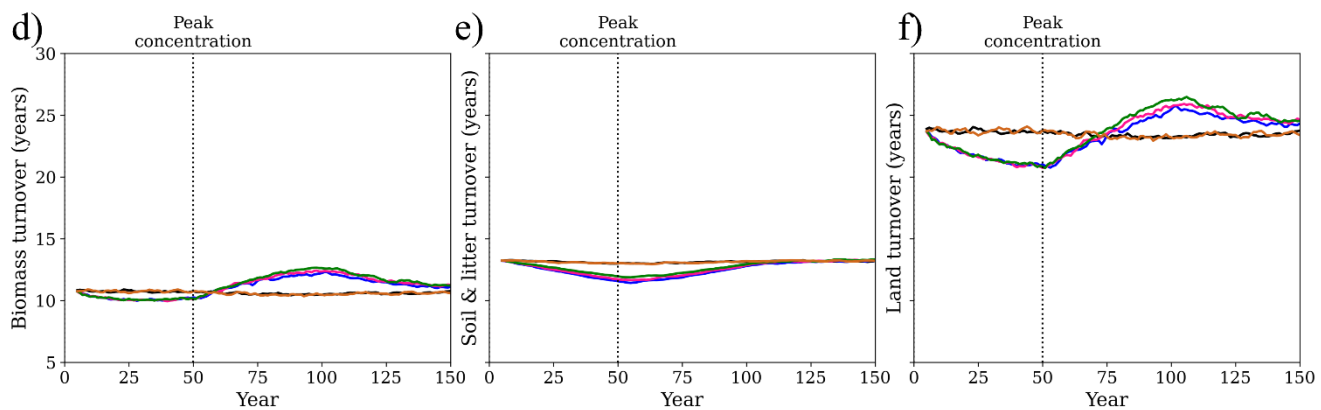
Figure S7 (continued). Global (a–c) GPP, (d–f) Ra and (g–i) Rh (GtC year^{-1}) as a function of (a, d, g) time (year), (b, e, h) CO_2 concentration (ppm) / CH_4 concentration (ppb, only for [nonCO$_2$]) and (c, f, i) GSAT (ºC) under selected scenarios.
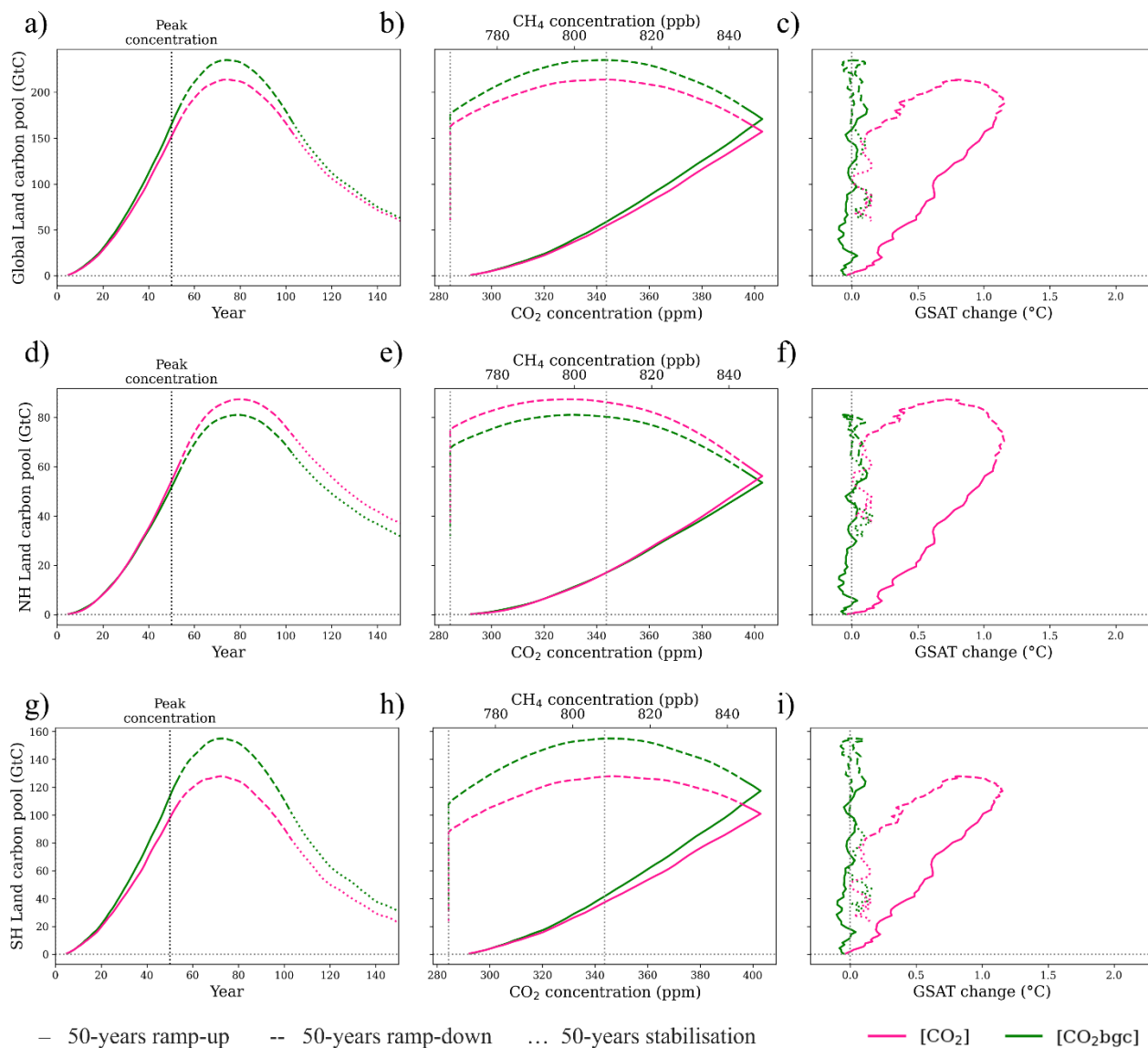
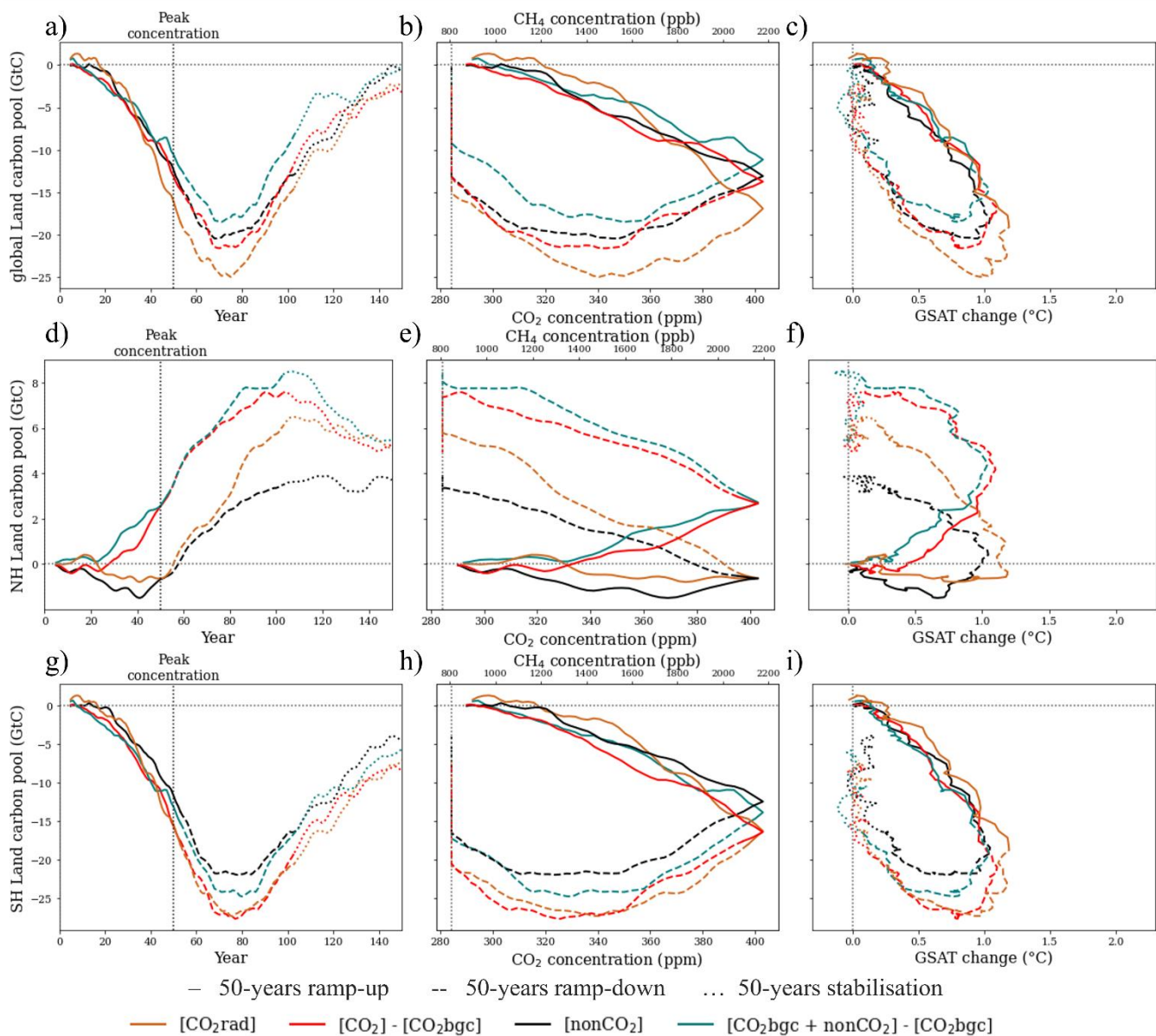## Northern high-latitude (>30º N)
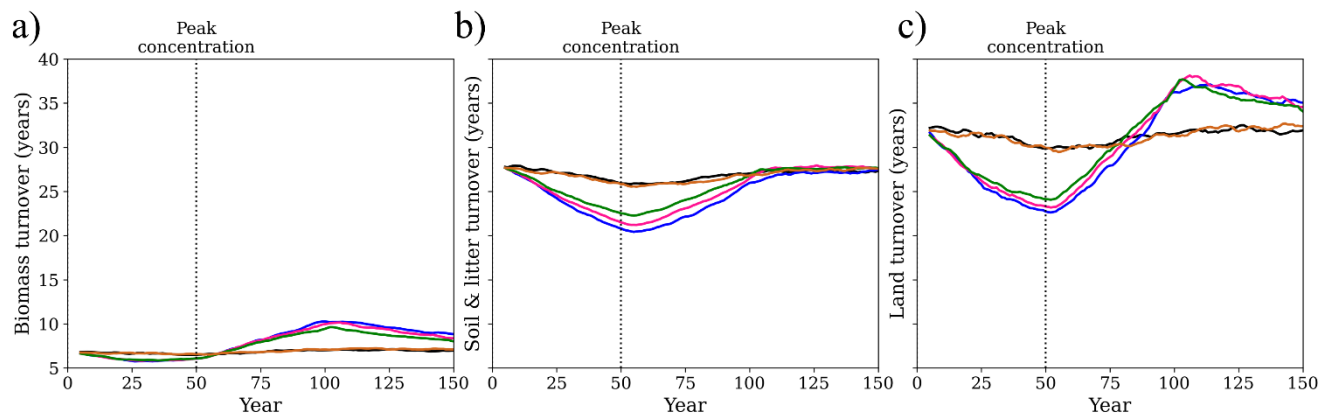
Subtropical and southern (<30º N)

Figure S8. (a, d) Biomass, (b, e) soil and litter and (c, f) land turnover time (years) over (a–c) northern high-latitude (>30º N) and (d–f) subtropical and southern (<30º N) under selected scenarios. Turnover is estimated as the ratio of carbon pool and net primary production. Estimates are shown for three-member ensemble means.
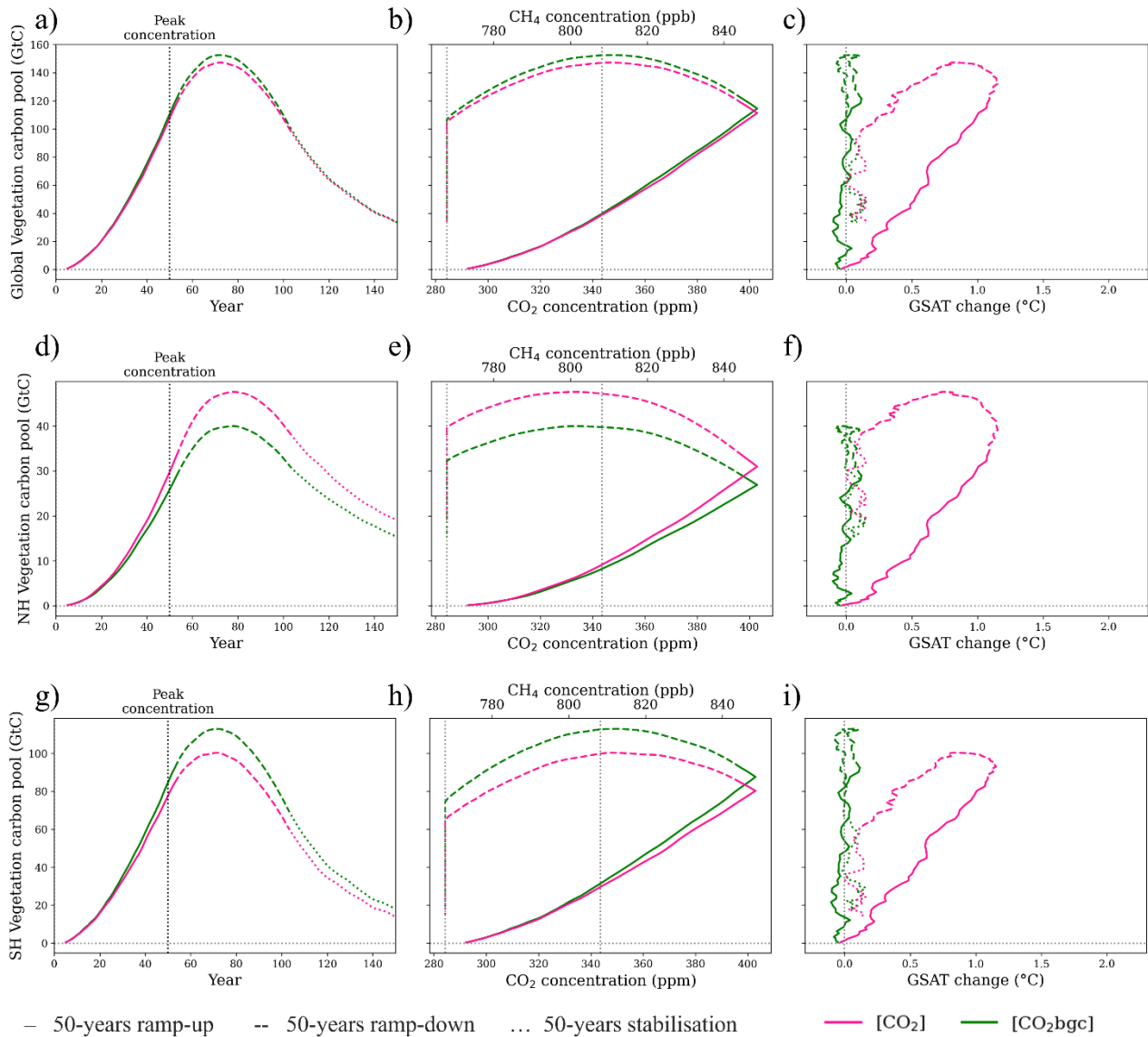
65

Figure S9. (a–c) Global, (d–f), northern high-latitude (>30º N) and (g–i) subtropical and southern (<30º N) net biome production, NBP (GtC year^{-1}), as a function of (a, d, g) time (year), (b, e, h) CO_2 concentration (ppm) / CH_4 concentration (ppb, only for [nonCO$_2$]) and (c, f, i) GSAT (ºC) under selected scenarios.

70

Figure S9 (continued). (a–c) Global, (d–f), northern high-latitude (>30° N) and (g–i) subtropical and southern (<30° N) net biome production, NBP (GtC year^{-1}), as a function of (a, d, g) time (year), (b, e, h) CO_2 concentration (ppm) / CH_4 concentration (ppb, only for [nonCO$_2$]) and (c, f, i) GSAT (°C) under selected scenarios.
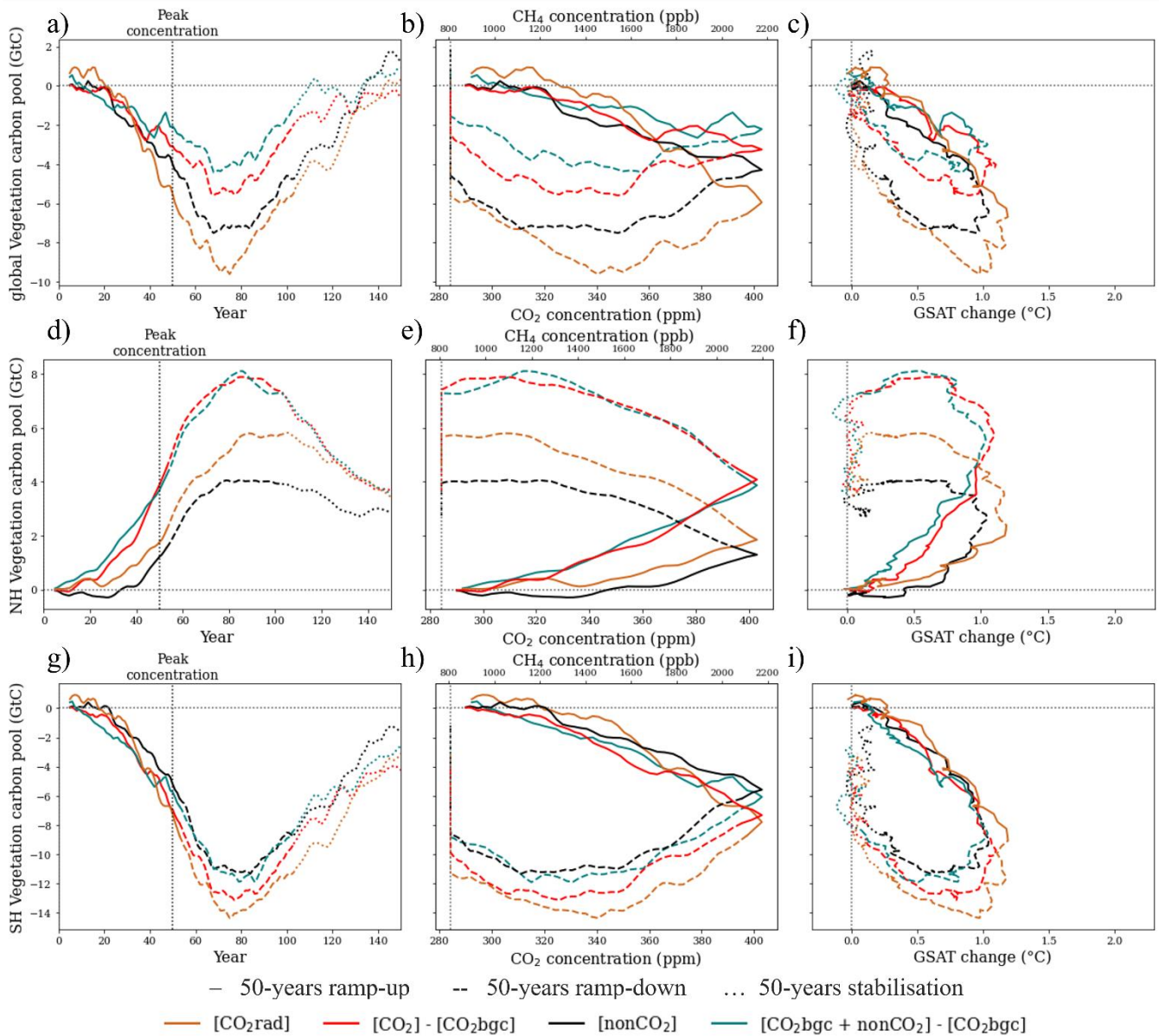
Figure S10. (a–c) Global, (d–f), northern high-latitude (>30º N) and (g–i) subtropical and southern (<30º N) changes in vegetation carbon pool (GtC), as a function of (a, d, g) time (year), (b, e, h) CO_2 concentration (ppm) / CH_4 concentration (ppb, only for [nonCO2]) and (c, f, i) GSAT (ºC) under selected scenarios.
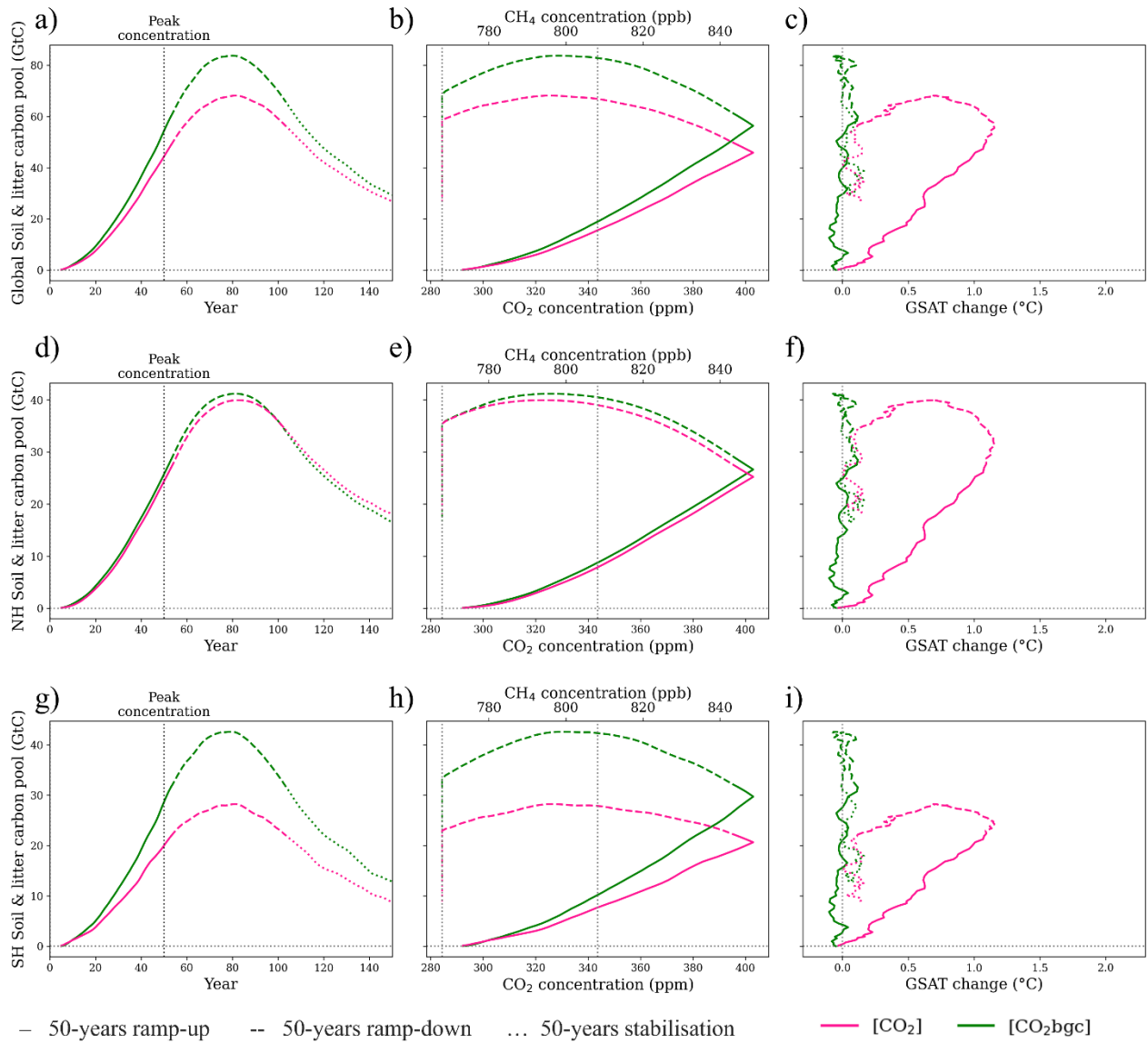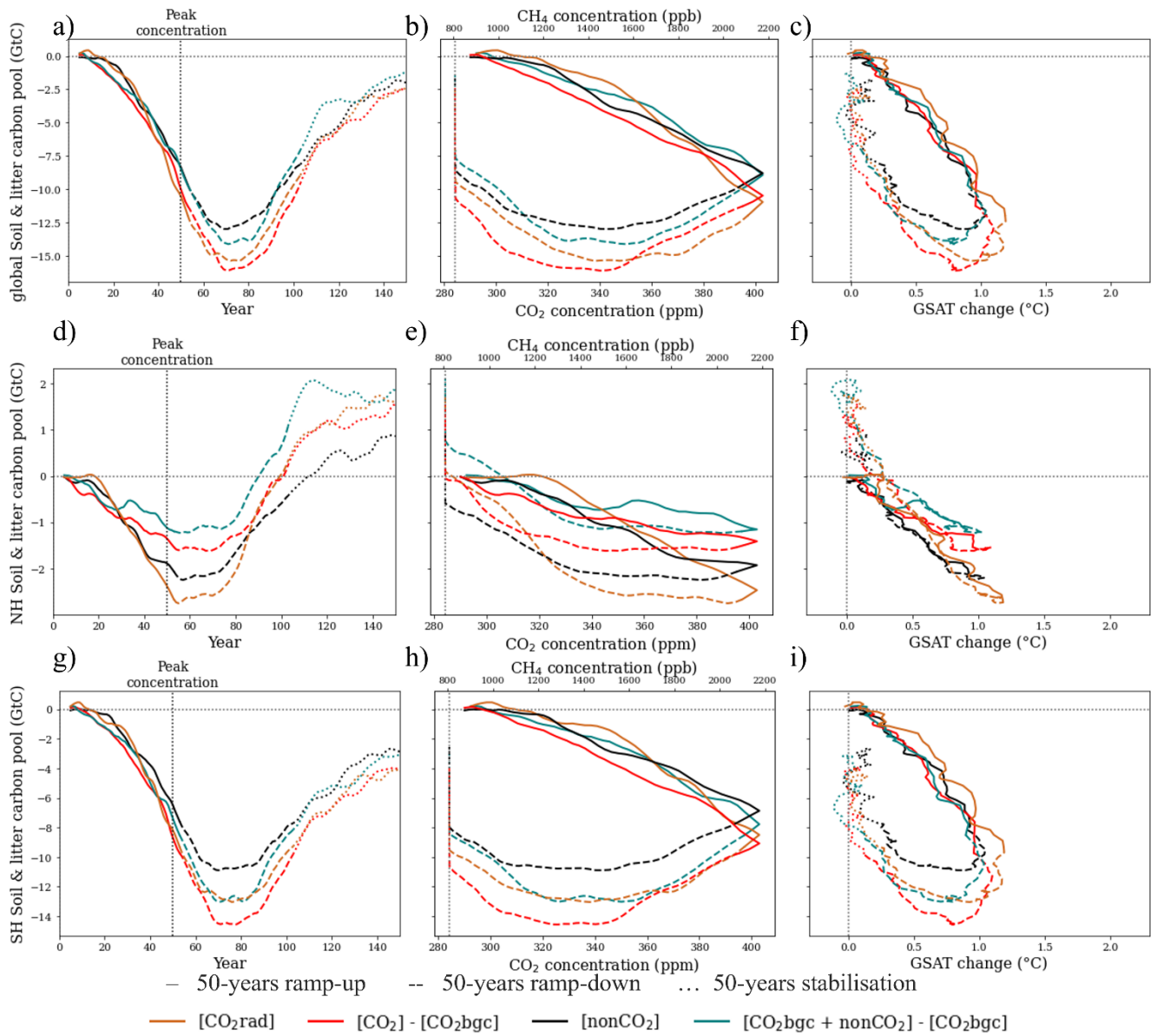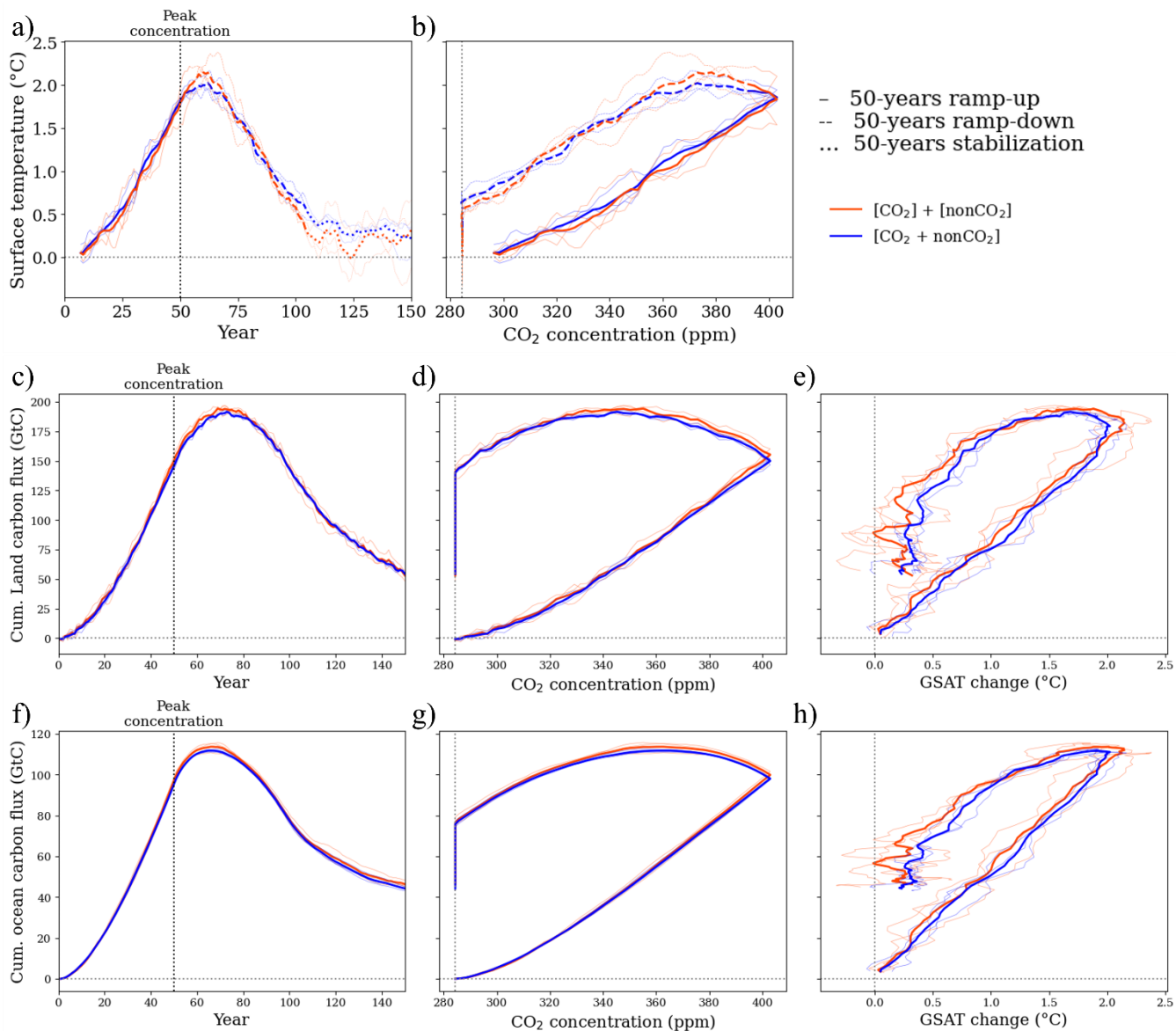
14

Figure S10 (continued). (a–c) Global, (d–f), northern high-latitude (>30º N) and (g–i) subtropical and southern (<30º N) changes in vegetation carbon pool (GtC), as a function of (a, d, g) time (year), (b, e, h) CO_2 concentration (ppm) / CH_4 concentration (ppb, only for [nonCO2]) and (c, f, i) GSAT (ºC) under selected scenarios.

Figure S11. (a–c) Global, (d–f), northern high-latitude (>30º N) and (g–i) subtropical and southern (<30º N) changes in soil and litter carbon pool (GtC), as a function of (a, d, g) time (year), (b, e, h) CO_2 concentration (ppm) / CH_4 concentration (ppb, only for [nonCO_2]) and (c, f, i) GSAT (ºC) under selected scenarios.

95   **Figure S11 (continued).** (a–c) Global, (d–f), northern high-latitude (>30º N) and (g–i) subtropical and southern (<30º N) changes in soil and litter carbon pool (GtC), as a function of (a, d, g) time (year), (b, e, h) CO_2 concentration (ppm) / CH_4 concentration (ppb, only for [nonCO₂]) and (c, f, i) GSAT (ºC) under selected scenarios.

100

Figure S12. Globally- and annually-averaged changes in (a, b) GSAT (°C), cumulative climate change-driven carbon fluxes (GtC) over (c–e) land and (f–h) ocean as a function of (a, c, f) time (year), (b, d, g) CO_2 concentration (ppm) and (e, h) GSAT (°C) under selected scenarios. The ramp-up, ramp-down and stabilisation periods for GSAT are indicated by different line styles. Thick lines indicate the ensemble means and thin lines correspond to three ensemble members.

18
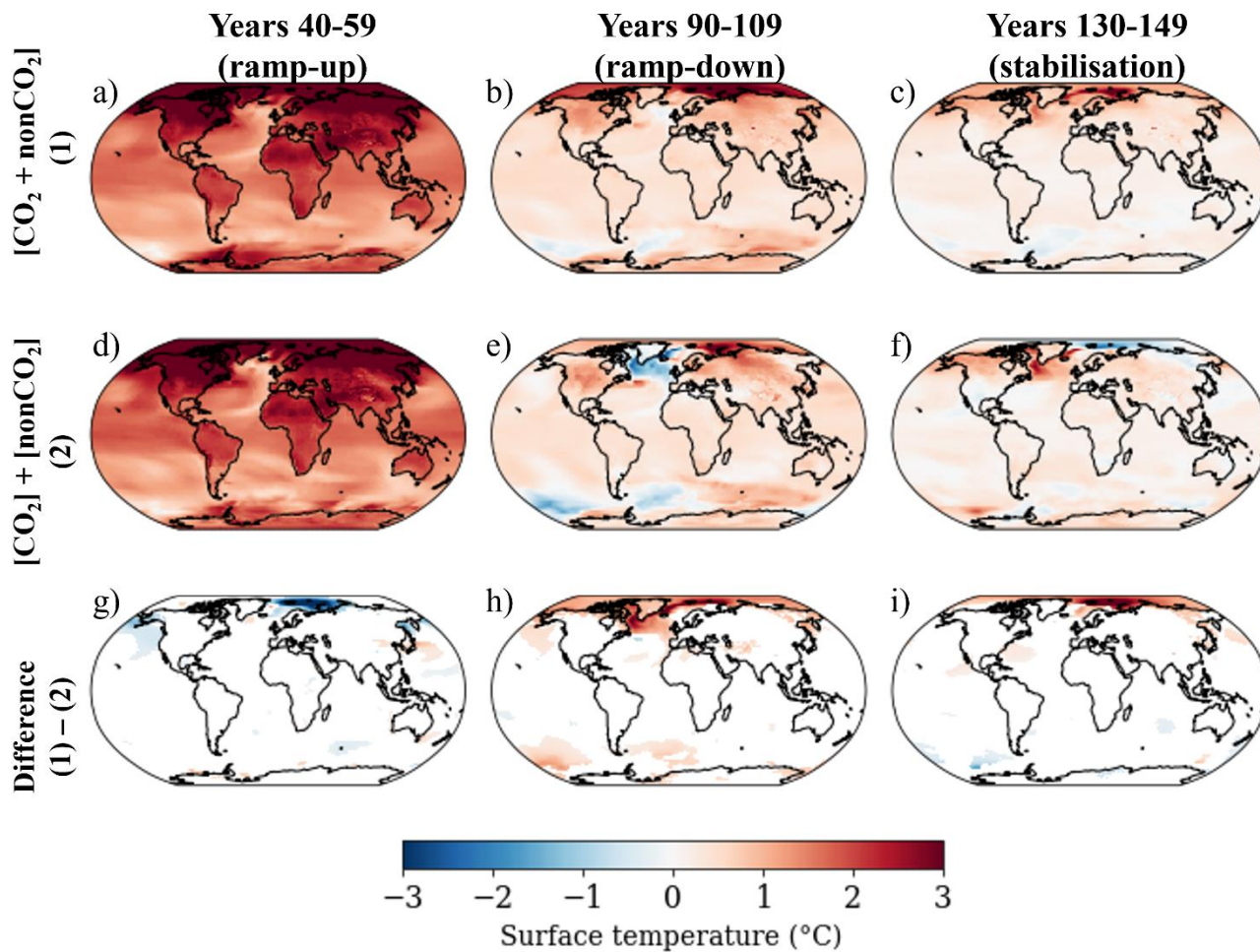
Figure S13. Spatial variation of three-member-ensemble mean changes in surface temperature (°C) averaged over 20 years at the end of (a, d, g) ramp-up, (b, e, h) ramp-down, and (c, f, i) stabilisation phases relative to piControl. For the differences between two scenarios (g, h, i), we draw only significantly different grids using three ensemble members ($p < 0.1$ based on t test, N=60).